Synthesis, Solid-State Structure and Solution Behavior of Hydrido-Bridged Adducts between the Group 11 $[M(PPh_3)]^+$ Cations and the Triangular Cluster Anion $[Re_3(\mu\text{-}H)_4(CO)_9(PPh_3)]^-$

Tiziana Beringhelli, Giuseppe D'Alfonso,* Maria Grazia Garavaglia, and Monica Panigati

Dipartimento di Chimica Inorganica, Metallorganica e Analitica, Via Venezian 21, 20133 Milano, Italy

Pierluigi Mercandelli* and Angelo Sironi

Dipartimento di Chimica Strutturale e Stereochimica Inorganica, Via Venezian 21, 20133 Milano, Italy

Received January 14, 2002

The reactions of the unsaturated anion $[Re_3(\mu\text{-}H)_4(CO)_9(PPh_3)]^-$ (**1**) with the metallic Lewis acids $[M(PPh_3)]^+$ (M = Cu, Ag, Au) afford the addition derivatives $[Re_3\{\mu\text{-}M(PPh_3)\}(\mu_3\text{-}H)(\mu\text{-}H)_3(CO)_9(PPh_3)]$, which have been characterized in solution and in the solid state, by X-ray analysis. The copper derivative is obtained also by reaction of $[Re_3(\mu\text{-}H)_3(\mu_3\text{-}H)(CO)_9]^-$ (as the $[Re(CO)_3(Me_2CO)_3]^+$ salt) with $[Cu(PPh_3)_2NO_3]$. Treatment with PPh_3 extrudes the $[M(PPh_3)]^+$ groups, restoring the starting anion **1**. Solid-state structures of the adducts show a butterfly Re_3M metal skeleton with one hydride bridging the Re_2M face and three hydrides spanning the three Re−Re edges. The interaction of the $[M(PPh_3)]^+$ cation with **1** leads only to a minor structural perturbation of the unsaturated $Re_2(\mu\text{-}H)_2$ moiety. The solid-state structure is maintained in nondonor solvents, while in acetone partial (Au, Ag) or complete (Cu) reversible ionic dissociation of the adducts is observed, affording **1** and solvated $[M(PPh_3)]^+$ cations. Experiments performed in different solvents show that the donor power and not the dielectric constant is the key factor responsible for dissociation. For the silver adduct the dissociation in acetone is fast on the NMR time scale. The exchange between **1** and the silver or copper (but not gold) adducts occurs even in CD_2Cl_2.

Introduction

Previous studies showed that the unsaturated triangular cluster anions $[Re_3(\mu\text{-}H)_4(CO)_9(L)]^-$ (46 valence electrons (VE's), L = two-electron donor)[1,2] easily react with electrophiles E^+ able to extract one hydride ligand and to promote the coordination of neutral L′ or anionic X^- ligands, affording saturated derivatives (48 VE's), according to eqs 1 and 2 (Scheme 1).[1−5] The most used

$$[Re_3(\mu\text{-}H)_4(CO)_9(L)]^- + E^+ + 2L' \rightarrow [Re_3(\mu\text{-}H)_3(CO)_9(L)(L')_2] + EH \quad (1)$$

$$[Re_3(\mu\text{-}H)_4(CO)_9(L)]^- + E^+ + X^- \rightarrow [Re_3(\mu\text{-}H)_3(\mu\text{-}X)(CO)_9(L)]^- + EH \quad (2)$$

electrophile E^+ was the proton, originating from either strong or weak Brønsted acids,[3] but also ethanolic iodine[4] or the tropylium ion[5] could be successfully used. Also, hydride transfer to the electrophilic carbon atom of organic molecules containing polarized multiple bonds was observed,[6,7] with coordination of the resulting anionic fragment on the cluster surface.

With other electrophiles (such as I_2 in nondonor solvents), oxidation of one hydride with hydrogen evolution was observed, instead of hydride transfer, according to eq 3 (L = CO).[4]

$$[Re_3(\mu\text{-}H)_4(CO)_9(L)]^- + 0.5I_2 \rightarrow [Re_3(\mu\text{-}H)_3(\mu\text{-}I)(CO)_9(L)]^- + 0.5H_2 \quad (3)$$

In all these cases, the thermodynamic site of the electrophilic attack was one of the hydrides of the $Re(\mu\text{-}H)_2Re$ moiety. According to a local electron counting, this is the site where not only the anionic charge

(1) Beringhelli, T.; Ciani, G.; D'Alfonso, G.; Molinari, H.; Sironi, A. *Inorg. Chem.* **1985**, *24*, 2666.
(2) Beringhelli, T.; Ciani, G.; D'Alfonso, G.; Freni, M.; Molinari, H.; Sironi, A. *J. Chem. Soc., Dalton Trans.* **1986**, 2691.
(3) (a) Ciani, G.; D'Alfonso, G.; Freni, M.; Romiti, P.; Sironi, A. *J. Organomet. Chem.* **1982**, *226*, C31. (b) Beringhelli, T.; Ciani, G.; D'Alfonso, G.; Freni, M.; Sironi, A. *J. Organomet. Chem.* **1982**, *244*, C27. (c) Ciani, G.; D'Alfonso, G.; Freni, M.; Romiti, P.; Sironi, A. *J. Organomet. Chem.* **1983**, *254*, C37. (d) Beringhelli, T.; Ciani, G.; D'Alfonso, G.; Freni, M.; Sironi, A. *J. Chem. Soc., Dalton Trans.* **1985**, 1507. (e) Beringhelli, T.; Ciani, G.; D'Alfonso, G.; Freni, M.; Moret, M.; Sironi, A. *J. Chem. Soc., Dalton Trans.* **1989**, 1143.
(4) Ciani, G.; D'Alfonso, G.; Freni, M.; Romiti, P.; Sironi, A. *Inorg. Chem.* **1983**, *22*, 3115.
(5) Beringhelli, T.; Ciani, G.; D'Alfonso, G.; Freni, M.; Romiti, P.; Sironi, A. *Inorg. Chem.* **1984**, *23*, 2849.
(6) Beringhelli, T.; Ciani, G.; D'Alfonso, G.; Freni, M.; Moret, M.; Sironi, A. *J. Organomet. Chem.* **1988**, *339*, 323.

10.1021/om0200252 CCC: $22.00
Publication on Web 05/25/2002

Scheme 1

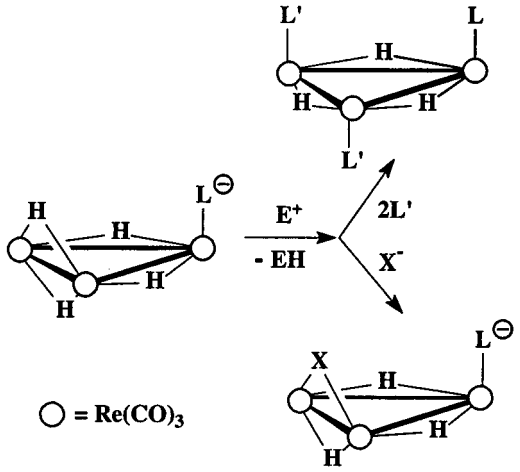

but also the unsaturation of the cluster is mainly localized. Therefore, such a moiety can be described either as an olefin-like system (containing a formal Re═Re double bond) or, better, as a diborane-like system (containing a four-center−four-electron bond).

We have now studied the reactions of the unsaturated anion $[Re_3(\mu\text{-}H)_4(CO)_9(PPh_3)]^-$ (**1**) with other electrophiles, namely the metallic Lewis acids $[M(PPh_3)]^+$, where M indicates a group 11 metal (Cu, Ag, Au). It is well-known that these cations are able to interact reversibly with transition metal hydrides, giving complexes containing one or more hydrides doubly or triply bridging between the transition and the coinage metal.[8−11] In particular, *addition* of $[M(PPh_3)]^+$ cations to rhenium polyhydrides was previously observed for the complexes $[ReH_5(PPh_3)_3]$,[12] $[ReH_5(PMe_2Ph)_3]$,[13] $[ReH_3(CO)(PMe_2Ph)_3]$,[14] $[Re_2H_8(PPh_3)_4]$,[15] and $[Re_3(\mu\text{-}H)_3(\mu_3\text{-ampy})(CO)_9]^-$ (Hampy = 2-amino-6-methylpyridine).[16] Particularly significant in this context is also the addition of $[M(PPh_3)]^+$ cations (M = Ag, Au) to the unsaturated species $[Mn_2(\mu\text{-}H)_2(CO)_6(\mu\text{-dppm})]$,[17] since it provided the first experimental evidence of a Lewis base behavior, toward group 11 cations, of an unsaturated *neutral* $M(\mu\text{-}H)_2M$ moiety.

In other cases, the reaction of transition-metal polyhydrides with $[M(PPh_3)]^+$ cations afforded substitution rather than addition, due to the isolobal relationship between H^+ and $[M(PPh_3)]^+$:[18,19] for instance, the reaction of $[Re_2H_8(PPh_3)_4]$ with $Au(PPh_3)NO_3$ afforded $[Re_2\{AuPPh_3\}_2H_6(PPh_3)_4]$.[20,21] In the case of $ReH_7(PPh_3)_2$, both substitution and addition were observed.[22]

On the other hand, the possibility that electron transfer rather than addition/substitution takes place cannot be ruled out a priori: in the reaction of $[Re_3(\mu\text{-}H)_4(CO)_{10}]^-$ with iodine the change from a donor to a nondonor solvent was sufficient to change the reaction course from hydride abstraction to redox. The relatively strong oxidizing ability of silver(I) toward metal hydride complexes is well-known.[23] Moreover, the reduction of $[Au(PPh_3)]^+$ with main-group or transition-metal hydrides has been used to promote the growth of large homo- or heteronuclear gold clusters: see, for instance, the reductions of $[Au(PPh_3)NO_3]$ with $NaBH_4$[24] or with $[ReH_7(PPh_3)_2]$,[22] affording, respectively, the $[Au_9(PPh_3)_8]^{3+}$ and $[(AuPPh_3)_5ReH_4(PPh_3)_2]^{2+}$ gold phosphine cluster cations.

It was therefore of interest to verify the preferred reaction path in the case of the anion **1**. We report here the complete solid-state and solution characterization of the 1:1 addition products $[Re_3\{\mu\text{-}M(PPh_3)\}(\mu_3\text{-}H)(\mu\text{-}H)_3(CO)_9(PPh_3)]$, which have been obtained for all three coinage metals, as well as the investigation of their stability in a donor solvent such as acetone.

Results and Discussion

Synthesis of the $[Re_3\{\mu\text{-}MPPh_3\}(\mu_3\text{-}H)(\mu\text{-}H)_3(CO)_9(PPh_3)]$ Complexes (M = Cu, Ag, Au). The treatment of the triangular cluster anion $[Re_3(\mu\text{-}H)_4(CO)_9(PPh_3)]^-$ (**1**), in CH_2Cl_2 solution, with an acetone solution containing a stoichiometric amount of PPh_3 and AgOTf (OTf = CF_3SO_3) caused an instantaneous shift toward higher frequencies of all the ν(CO) bands (ca. 10−15 cm^{-1}; see Table 1). Standard workup (see Experimental Section) led to the isolation of a sun yellow compound, characterized as the complex $[Re_3\{\mu\text{-}AgPPh_3\}(\mu_3\text{-}H)(\mu\text{-}H)_3(CO)_9(PPh_3)]$ (**2**) on the basis of its spectroscopic data and of a single-crystal X-ray analysis (Scheme 2, eq 4, M = Ag).

$$[Re_3(\mu\text{-}H)_4(CO)_9(PPh_3)]^- + [MPPh_3]^+ \rightarrow [Re_3\{\mu\text{-}MPPh_3\}(\mu_3\text{-}H)(\mu\text{-}H)_3(CO)_9(PPh_3)] \quad (4)$$

The presence of a phosphine bound to the silver atom (P(2) in Table 1) was revealed by the two doublets in the ^{31}P NMR spectrum arising from the coupling with ^{109}Ag and ^{107}Ag, while the phosphine bound to a vertex of the Re cluster, labeled P(1), was responsible for a singlet at a δ value quite similar to that of the starting anion **1**. The three hydridic resonances in the ratio 1:1:2

(7) (a) Beringhelli, T.; Ciani, G.; D'Alfonso, G.; Freni, M.; Moret, M.; Sironi, A. *J. Organomet. Chem.* **1990**, *399*, 291. (b) Beringhelli, T.; Ciani, G.; D'Alfonso, G.; Minoja, A. P.; Moret, M.; Sironi, A. *Organometallics* **1991**, *10*, 3131.

(8) (a) Salter, I. D. In *Comprehensive Organometallic Chemistry II*; Abel, E. W., Stone, F. G. A., Wilkinson, G., Eds.; Pergamon: Oxford, U.K., 1995; Vol. 10, p 255. (b) Salter, I. D. *Adv. Organomet. Chem.* **1989**, *29*, 249.

(9) (a) Mingos, D. M. P.; Watson, M. J. *Adv. Inorg. Chem.* **1992**, *39*, 327. (b) Hall, K. P.; Mingos, D. M. P. *Prog. Inorg. Chem.* **1984**, *32*, 237.

(10) Chetcuti, M. J. In *Comprehensive Organometallic Chemistry II*; Abel, E. W., Stone, F. G. A., Wilkinson, G., Eds.; Pergamon: Oxford, U.K., 1995; Vol. 10, p 23.

(11) Albinati, A.; Venanzi, L. M. *Coord, Chem. Rev.* **2000**, *200−202*, 687.

(12) Moehring, G. A.; Walton, R. A. *J. Chem. Soc., Dalton Trans.* **1988**, 1701.

(13) Sutherland, B. R.; Folting, K.; Streib, W. E.; Ho, D. M.; Huffman, J. C.; Caulton, K. G. *J. Am. Chem. Soc.* **1987**, *109*, 3489.

(14) Luo, S.; Burns, C. J.; Kubas, G. J.; Bryan, J. C.; Crabtree, R. H. *J. Cluster Sci.* **2000**, *11*, 189.

(15) Moehring, G. A.; Fanwick, P. E.; Walton, R. A. *Inorg. Chem.* **1987**, *26*, 1861.

(16) Cabeza, J. A.; Riera, V.; Trivedi, R.; Grepioni, F. *Organometallics* **2000**, *19*, 2043.

(17) Carreno, R.; Riera, V.; Ruiz, M. A.; Bois, C.; Jeannin, Y. *Organometallics* **1992**, *11*, 2923.

(18) Evans, D. G.; Mingos, D. M. P. *J. Organomet. Chem.* **1982**, *232*, 171.

(19) Lauher, J. W.; Wald, K. *J. Am. Chem. Soc.* **1981**, *103*, 7648.

(20) Boyle, P. D.; Johnson, B. J.; Alexander, B. D.; Casalnuovo, J. A.; Gannon, P. R.; Johnson, S. M.; Larka, E. A.; Mueting, A. M.; Pignolet, L. H. *Inorg. Chem.* **1987**, *26*, 1346.

(21) See also: Casalnuovo, A. L.; Pignolet, L. H.; van der Velden, J. W. A.; Bour, J. J.; Steggerda, J. J. *J. Am. Chem. Soc.* **1983**, *105*, 5957.

(22) Boyle, P. D.; Johnson, B. J.; Buehler, A.; Pignolet, L. H. *Inorg. Chem.* **1986**, *25*, 5.

(23) See for instance: (a) Rhodes, L. F.; Zubkowski, J. D.; Folting, K.; Huffman, J. C.; Caulton, K. G. *Inorg. Chem.* **1982**, *21*, 4185. (b) Rhodes, L. F.; Huffman, J. C.; Caulton, K. G. *Inorg. Chim. Acta* **1992**, *198−200*, 639.

(24) Cariati, F.; Naldini, L. *J. Chem. Soc., Dalton Trans.* **1972**, 2286.

Table 1. IR and NMR Data for the Title Compounds (Room Temperature, CD_2Cl_2)

compd	$\delta(H_a)$ (ppm) (J_{HP}, Hz)	$\delta(H_b)$ (ppm) (J_{HP}, Hz)	$\delta(H_c)$ (ppm) (J_{HP}, Hz)	$\delta(P(1))$ (ppm)	$\delta(P(2))$ (ppm)	IR (ν_{CO}) (cm^{-1})
1	−7.73 (d, 1H; 5.6)	−8.91 (s, 1H)	−12.26 (d, 2H; 16.2)	8.1		2032 m, 2003 s, 1996 s, 1926 sh, 1906 s
2	−8.55 (d, 1H; 4.1)	−10.82 (dd, 1H; 31)[a]	−11.92 (d, 2H; 16.3)	10.3	24.0[b]	2046 m, 2015 vs, 1949 m, 1934 m, 1921 ms
3	−8.30 (d, 1H; 4.3)	−7.62 (d, 1H; 70)	−11.15 (d, 2H; 16.1)	9.0	59.3	2047 m, 2016 vs, 1950 m, 1936 m 1925 m, sh
4	−8.24 (s, 1H)	−11.84(d, 1H; 27)	−11.31 (d, 2H; 15.8)	9.4	14.4	2048 m, 2017 vs, 1954 m, 1935 m, 1921 m

[a] $^1J_{HAg} = 85$ Hz. [b] dd, $^1J_{AgP} = 645$ and 560 Hz.

Scheme 2[a]

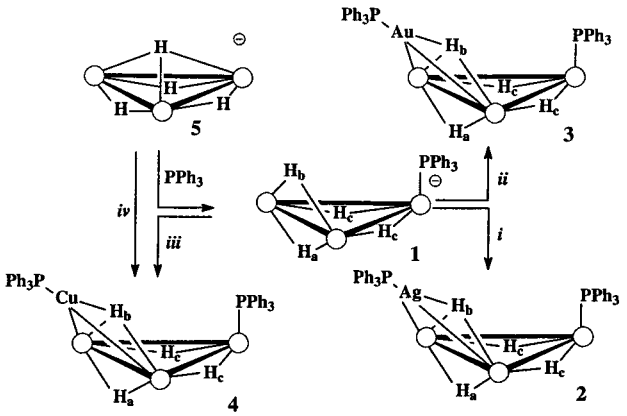

[a] Legend: (i) AgOTf + PPh_3; (ii) $AuCl(PPh_3)$; (iii) $Cu(NCMe)_4^+ + PPh_3$; (iv) $Cu(PPh_3)_2(NO_3)$.

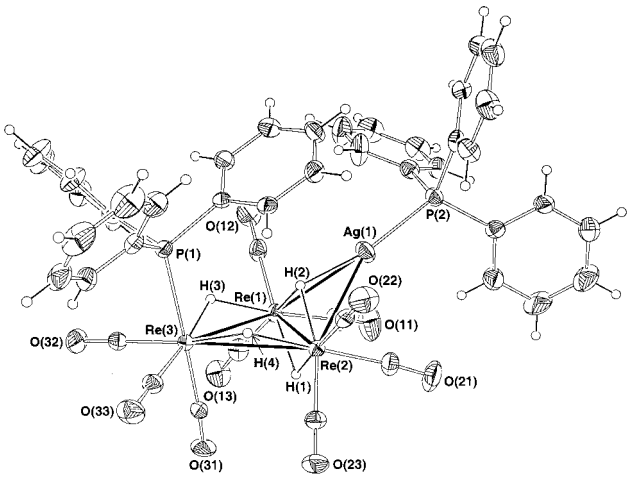

Figure 1. ORTEP drawing of $[Re_3\{\mu\text{-}Ag(PPh_3)\}(\mu_3\text{-}H)(\mu\text{-}H)_3(CO)_9(PPh_3)]$ (**2**) with a partial labeling scheme. Thermal ellipsoids are drawn at the 30% probability level. Hydrogen atoms are given arbitrary radii.

(see Table 1) in ^1H NMR spectrum indicated the preservation of the C_s symmetry of the starting anion **1**. Variable-temperature analysis down to 203 K, in CD_2Cl_2, did not show any significant change. One of the signals of intensity 1 (−10.82 ppm) appeared as a doublet of doublets, due to coupling both with silver and phosphorus atoms (the signal was too broad to allow us to resolve the couplings with ^{109}Ag and ^{107}Ag, even in a ^{31}P-decoupled spectrum): the high value of J_{HAg} (85 Hz) indicated that the hydride responsible for this signal (labeled as H_b in Table 1) was directly bound to the silver atom. The other two hydridic resonances had chemical shift and J_{HP} values close to those of **1**, indicating that they had been little affected by the addition of the silver cation. A 2D NOESY experiment performed in CD_2Cl_2 at room temperature showed that all the hydride resonances but that at −8.55 ppm had NOE cross-peaks with the protons of the two phosphines: this indicated that the hydride responsible for this resonance, labeled as H_a in Scheme 2, is coordinated in an anti position with respect to both the $Ag(PPh_3)$ and PPh_3 ligands. This means that the $Ag(PPh_3)$ fragment is syn with respect to the rhenium-bound PPh_3 ligand.

These data, as well as the results of the $^1H-^{31}P$ 2D HMQC experiment described in the Experimental Section, agree with the solid-state structure of **2**, depicted in Figure 1.

The analogous gold derivative was obtained according to the same reaction 4 (M = Au), by treating the anion **1** with a stoichiometric amount of the $[Au(PPh_3)]^+$ cation (prepared in situ from $Au(PPh_3)Cl$ and AgOTf). Also in this case the reaction was instantaneous and the same purification procedure afforded a bright orange compound, formulated as $[Re_3\{\mu\text{-}Au(PPh_3)\}(\mu_3\text{-}H)(\mu\text{-}H)_3(CO)_9(PPh_3)]$ (**3**) on the basis of its IR and NMR data (Table 1). The large value of J_{HP} for the triply bridging hydride (70 Hz) agrees with previous literature data for complexes containing analogous $M_2(\mu_3\text{-}H)(\mu\text{-}AuPPh_3)$ fragments with an approximately *transoid* arrangement of the hydride and the phosphine ligands around the gold atom (M = Mn, 74 Hz;[17] M = Mo, 86 Hz;[25] M = Re, 59 Hz[16]).[26] Selective $\{^{31}P\}-^1H$ decoupling experiments confirmed that also in this case the ^{31}P resonance at high field was due to the phosphine ligand bound to the rhenium cluster. The solid-state structure determined from a single-crystal X-ray analysis is depicted in Figure 2.

To obtain the corresponding copper derivative according to reaction 4, we treated the anion **1** with a CH_2Cl_2 solution containing stoichiometric amounts of PPh_3 and $[Cu(CH_3CN)_4]BF_4$. The NMR data of the main reaction product (Table 1) confirmed the formation of the expected derivative $[Re_3\{\mu\text{-}Cu(PPh_3)\}(\mu_3\text{-}H)(\mu\text{-}H)_3(CO)_9(PPh_3)]$ (**4**), whose solid-state structure is shown in Figure S2 (Supporting Information). In this case, however, the NMR spectrum of the isolated yellow microcrystalline solid showed, besides the signals of **4**, also some unattributed hydridic resonances (the main one being a doublet at −6.43 ppm, with $J_{HP} = 16$ Hz), whose overall intensity varied in the range 18−35% in repeated preparations with slightly different experimental procedures.

When the reaction was performed directly in the NMR tube, the ^1H spectra showed the formation of a species containing one or more MeCN molecules bound to the

(25) Ferrer, M.; Reina, R.; Rossel, O.; Seco, M.; Alvarez, S.; Ruiz, E.; Pellinghelli, M. A.; Tiripicchio, A. *Organometallics* **1992**, *11*, 3753.

(26) Still higher values have been observed for transoid doubly bridging hydrides in $M(\mu\text{-}H)(\mu\text{-}AuPPh_3)$ fragments: M = Cr, 105 Hz;[27] M = Re, 96 Hz.[14]

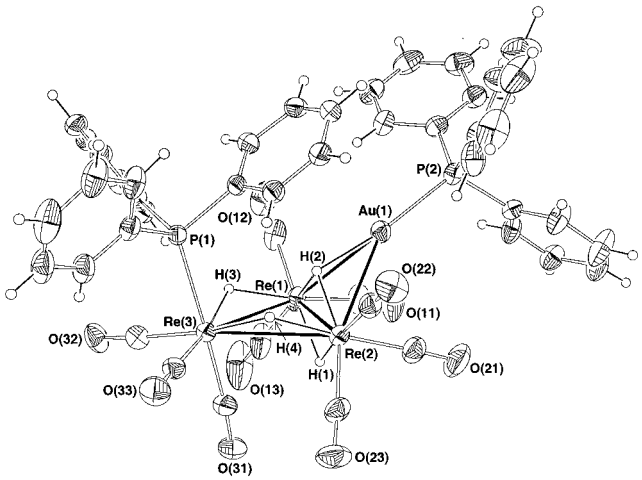

Figure 2. ORTEP drawing of $[Re_3\{\mu\text{-}Au(PPh_3)\}(\mu_3\text{-}H)(\mu\text{-}H)_3(CO)_9(PPh_3)]$ (**3**) with a partial labeling scheme. Thermal ellipsoids are drawn at the 30% probability level. Hydrogen atoms are given arbitrary radii.

Cu atom (see the Supporting Information). The same $[Re_3\{\mu\text{-}Cu(PPh_3)(NCMe)_n\}(\mu_3\text{-}H)(\mu\text{-}H)_3(CO)_9(PPh_3)]$ species was obtained upon treating **4** with MeCN.

To obtain a more selective pathway to compound **4**, we attempted two different synthetic approaches. At first we tried to generate the $[Cu(PPh_3)]^+$ cation by treating $[Cu(PPh_3)Cl]_4$ with AgOTf, as in the synthesis of the gold derivative **3**. However, the ^{1}H NMR spectrum revealed the formation of a complex mixture of hydridic derivatives in which compound **4** was only a minor component. Then we explored a fully different approach, consisting of the reaction of the complex $[Cu(PPh_3)_2(NO_3)]$ with the "super-unsaturated" (44 VE's) anion $[Re_3(\mu\text{-}H)_3(\mu_3\text{-}H)(CO)_9]^-$ (**5**),[28] as shown in Scheme 2. This approach (eq 5) was successful only on using the $[Re(CO)_3(Me_2CO)_3]^+$ salt of **5** (generated through the reaction of $[Re_4(\mu_3\text{-}H)_4(CO)_{12}]$ with acetone, according to eq 6).[28a,29] When the reaction was repeated by using

$$[Re_3(\mu\text{-}H)_3(\mu_3\text{-}H)(CO)_9]^- + [Cu(PPh_3)_2(NO_3)] \rightarrow [Re_3\{\mu\text{-}Cu(PPh_3)\}(\mu_3\text{-}H)(\mu\text{-}H)_3(CO)_9(PPh_3)] + NO_3^- \quad (5)$$

$$[Re_4(\mu_3\text{-}H)_4(CO)_{12}] + 3Me_2CO \rightarrow [Re_3(\mu\text{-}H)_3(\mu_3\text{-}H)(CO)_9]^- + [Re(CO)_3(Me_2CO)_3]^+ \quad (6)$$

the PPh_4^+ salt of **5**, the formation of **4** was negligible, the anion **1** being the main reaction product, both in CH_2Cl_2 and in THF solution. We suppose that the $[Re(CO)_3(Me_2CO)_3]^+$ cation formed in reaction 6 plays a key role in the activation of the $[Cu(PPh_3)_2(NO_3)]$ reactant, by abstracting the NO_3^- anion and generating the copper cation able to attack the rhenium hydrido carbonyl cluster anion (eq 7).

$$[Re(CO)_3(Me_2CO)_3]^+ + [Cu(PPh_3)_2(NO_3)] \rightarrow [Re(CO)_3(Me_2CO)_2(NO_3)] + [Cu(PPh_3)_2]^+ + Me_2CO \quad (7)$$

(27) Green, M.; Orpen, A. G.; Salter, I. D.; Stone, F. G. A. *J. Chem. Soc., Dalton Trans.* **1984**, 2497.

It is worth noting that the *preliminary* fragmentation of $[Re_4(\mu_3\text{-}H)_4(CO)_{12}]$ (eq 6) was not necessary: the simultaneous treatment of $[Re_4(\mu_3\text{-}H)_4(CO)_{12}]$ with 1 equiv of $[Cu(PPh_3)_2(NO_3)]$ and some acetone (30 μL), in CD_2Cl_2 at low temperature afforded adduct **4** as the only hydridic species. Under these conditions, ^{1}H NMR monitoring showed the intermediate formation of a species responsible for two hydridic resonances (ratio 1:1, δ −9.42, −11.20 ppm, at 193 K), which at 243 K gave rise to an averaged signal at δ −10.20. After 2 h at 253 K this species was completely transformed into **4**.

In agreement with these findings, no reaction was observed between **1** and the neutral species $[M(PPh_3)Cl]$ (M = Cu, Ag, Au).

Solid State Structure of the Addition Derivatives $[Re_3\{\mu\text{-}M(PPh_3)\}(\mu_3\text{-}H)(\mu\text{-}H)_3(CO)_9(PPh_3)]$ (2−4). The molecular structures of compounds **2**−**4** were determined by X-ray diffraction analysis. The copper derivative **4** crystallizes in two polymorphic forms, a monoclinic and an orthorhombic one (**4m** and **4o**), isomorphous with the silver and the gold derivatives **2** and **3**, respectively (see Table 4). Figures 1 and 2 show ORTEP drawings of **2** and **3**, respectively. Table 2 contains the most relevant bond distances and angles for **2**−**4**, while Table 3 collects some mean bond parameters for the adducts **2**−**4** and for the parent compound $[Re_3(\mu\text{-}H)_4(CO)_9(PPh_3)]^-$ (**1**).

Compounds **2**−**4** exhibit a Re_3M butterfly metal core with all the Re−Re edges and the Re_2M face bridged by one hydrido ligand. Each of the rhenium atoms also bears three terminal CO ligands with facial coordination; one triphenylphosphine ligand is bound to Re(3) (in an axial position) and another one to M(1) (in a *transoid* arrangement with respect to the face-bridging hydride).

Ignoring the propeller-like conformation adopted by the two triphenylphosphine ligands, molecules **2**−**4** (as well as the parent anion **1**) show an approximate C_s symmetry, the main deviation being related to the distorted trigonal coordination of the group 11 metal atom, in the monoclinic phases **2** and **4m** (compare the angles Re(1)−M(1)−P(2) and Re(2)−M(1)−P(2) in Table 2).

With reference to the parent anion **1** the Re−Re edge originally bridged by two hydrides is now additionally spanned by a μ-$MPPh_3$ group. As a consequence of the larger size of the bridgehead atom (a group 11 metal vs hydrogen), the Re(1)−Re(2) bond distance results slightly lengthened in **2**−**4** with respect to **1** (the effect is stronger for the more hindered gold derivative; see Table 3). The main effect on the overall stereochemistry of the addition of the $MPPh_3$ fragment is a displacement of the carbonyl ligands on Re(1) and Re(2) away from this sterically demanding group: in particular the Re(1,2)−Re(2,1)−C(diagonal) angles are increased for the carbonyl ligands lying on the same side of the Re_3 plane bearing the $MPPh_3$ group (C(12) and C(22)) and are decreased for those on the opposite side (C(13) and C(23)), with respect to the values in the parent anion **1**

(28) (a) Beringhelli, T.; D'Alfonso, G. *J. Chem. Soc., Chem. Commun.* **1994**, 2631. (b) Horng, H. C.; Cheng, C. P.; Yang, C. S.; Lee, G.-H. *Organometallics* **1996**, *15*, 2543.

(29) Beringhelli, T.; D'Alfonso, G.; Garavaglia, M. G. *J. Chem. Soc., Dalton Trans.* **1996**, 1771.

Table 2. Selected Bond Distances (Å) and Angles (deg) for the Addition Derivatives $[Re_3\{\mu\text{-}M(PPh_3)\}(\mu_3\text{-}H)(\mu\text{-}H)_3(CO)_9(PPh_3)]$

	2 (M = Ag)	**3** (M = Au)	**4m** (M = Cu)	**4o** (M = Cu)
Re(1)−Re(2)	2.8398(9)	2.8589(7)	2.8269(15)	2.8256(7)
Re(1)−Re(3)	3.1821(9)	3.2003(7)	3.1817(10)	3.2115(8)
Re(2)−Re(3)	3.2166(8)	3.1854(7)	3.2161(9)	3.1796(8)
Re(1)−M(1)	3.0145(9)	2.9673(6)	2.8007(11)	2.8024(13)
Re(2)−M(1)	2.9604(9)	2.9260(6)	2.7425(11)	2.7437(13)
Re(1)−C(11)	1.933(8)	1.939(7)	1.932(7)	1.909(11)
Re(1)−C(12)	1.927(8)	1.935(9)	1.925(7)	1.922(12)
Re(1)−C(13)	1.922(8)	1.921(8)	1.907(7)	1.916(13)
Re(2)−C(21)	1.922(7)	1.936(8)	1.924(7)	1.915(12)
Re(2)−C(22)	1.928(8)	1.934(8)	1.931(7)	1.910(12)
Re(2)−C(23)	1.903(7)	1.902(7)	1.946(7)	1.918(12)
Re(3)−C(31)	1.910(7)	1.899(7)	1.925(7)	1.905(10)
Re(3)−C(32)	1.917(7)	1.936(7)	1.925(7)	1.936(12)
Re(3)−C(33)	1.945(7)	1.925(7)	1.959(7)	1.911(12)
Re(3)−P(1)	2.4958(17)	2.4793(15)	2.4956(19)	2.474(2)
M(1)−P(2)	2.3935(19)	2.2822(16)	2.2127(18)	2.214(3)
P(1)−C(41)	1.822(6)	1.833(6)	1.830(6)	1.822(8)
P(1)−C(47)	1.810(7)	1.836(6)	1.824(6)	1.839(9)
P(1)−C(53)	1.826(7)	1.836(6)	1.840(6)	1.849(8)
P(2)−C(59)	1.824(7)	1.807(6)	1.823(6)	1.810(9)
P(2)−C(65)	1.814(7)	1.824(6)	1.817(6)	1.814(9)
P(2)−C(71)	1.840(7)	1.820(7)	1.831(6)	1.825(9)
Re(2)−Re(1)−Re(3)	64.278(10)	63.135(16)	64.404(12)	63.183(18)
Re(1)−Re(2)−Re(3)	63.031(16)	63.673(16)	63.15(2)	64.341(18)
Re(1)−Re(3)−Re(2)	52.69(2)	53.192(9)	52.44(3)	52.476(13)
Re(2)−Re(1)−M(1)	60.664(18)	60.259(13)	58.33(3)	58.35(3)
Re(1)−Re(2)−M(1)	62.589(18)	61.707(10)	60.36(3)	60.40(3)
Re(3)−Re(1)−M(1)	109.09(2)	105.759(19)	111.69(3)	108.67(3)
Re(3)−Re(2)−M(1)	109.57(3)	107.153(18)	112.28(4)	111.13(3)
Re(1)−M(1)−Re(2)	56.75(2)	58.034(16)	61.31(3)	61.25(3)
Re(2)−Re(1)−C(11)	99.7(2)	100.9(2)	101.2(2)	100.8(3)
Re(2)−Re(1)−C(12)	138.7(2)	139.8(2)	139.6(2)	138.6(3)
Re(2)−Re(1)−C(13)	129.6(2)	126.8(3)	128.9(2)	130.3(5)
Re(3)−Re(1)−C(11)	158.5(2)	160.8(3)	160.0(2)	160.4(3)
Re(3)−Re(1)−C(12)	110.7(2)	110.4(2)	109.5(2)	109.8(3)
Re(3)−Re(1)−C(13)	91.4(2)	91.3(3)	90.9(2)	93.9(4)
M(1)−Re(1)−C(11)	71.1(2)	71.7(2)	66.9(2)	67.4(3)
M(1)−Re(1)−C(12)	86.0(2)	87.0(2)	92.9(2)	90.6(3)
M(1)−Re(1)−C(13)	159.2(2)	162.2(2)	154.9(2)	155.9(3)
Re(1)−Re(2)−C(21)	99.1(2)	97.1(2)	100.1(2)	97.5(3)
Re(1)−Re(2)−C(22)	139.11(19)	140.63(19)	138.9(2)	139.8(3)
Re(1)−Re(2)−C(23)	131.5(2)	129.7(2)	132.24(18)	131.2(3)
Re(3)−Re(2)−C(21)	156.7(2)	155.2(2)	156.8(2)	155.9(4)
Re(3)−Re(2)−C(22)	112.7(2)	114.2(2)	112.8(2)	113.1(3)
Re(3)−Re(2)−C(23)	93.5(2)	91.5(2)	92.65(19)	91.4(3)
M(1)−Re(2)−C(21)	70.5(2)	73.2(2)	67.0(2)	68.2(3)
M(1)−Re(2)−C(22)	84.1(2)	84.14(19)	88.8(2)	87.4(3)
M(1)−Re(2)−C(23)	156.9(2)	161.3(2)	154.20(19)	157.0(3)
Re(1)−Re(3)−C(31)	109.0(2)	108.04(19)	108.2(2)	110.3(3)
Re(1)−Re(3)−C(32)	155.3(2)	157.2(2)	155.62(19)	156.8(3)
Re(1)−Re(3)−C(33)	77.67(18)	81.6(2)	78.66(18)	83.0(3)
Re(1)−Re(3)−P(1)	99.31(4)	97.84(4)	99.33(4)	95.72(5)
Re(2)−Re(3)−C(31)	160.2(2)	158.2(2)	159.2(2)	160.0(3)
Re(2)−Re(3)−C(32)	105.7(2)	104.9(2)	106.1(2)	104.7(3)
Re(2)−Re(3)−C(33)	81.32(18)	77.3(2)	81.94(18)	78.1(3)
Re(2)−Re(3)−P(1)	101.61(4)	105.12(4)	101.73(4)	104.12(5)
Re(1)−M(1)−P(2)	135.84(5)	146.08(4)	137.49(6)	146.58(8)
Re(2)−M(1)−P(2)	156.49(5)	147.43(4)	158.01(6)	148.29(9)
Re(3)−P(1)−C(41)	115.77(19)	114.89(19)	115.11(19)	114.6(3)
Re(3)−P(1)−C(47)	115.4(2)	115.0(2)	115.4(2)	115.3(3)
Re(3)−P(1)−C(53)	114.2(2)	116.2(2)	113.9(2)	116.1(3)
M(1)−P(2)−C(59)	116.6(2)	112.8(2)	117.8(2)	114.3(3)
M(1)−P(2)−C(65)	114.7(2)	112.5(2)	115.0(2)	113.6(3)
M(1)−P(2)−C(71)	108.7(2)	111.7(2)	109.0(2)	111.1(3)

(see Table 3). The effect is, as expected, slightly more marked for the gold derivative than for the silver and copper ones. However, the data reported in Table 3 clearly show that the interaction of the parent anion **1** with the group 11 metal phosphine group results only in a minor structural perturbation of the $Re_2(\mu\text{-}H)_2$ moiety.

In compounds **2**−**4** the bridging $MPPh_3$ group and the rhenium-bound triphenylphosphine lay on the same side of the Re_3 plane, in a syn arrangement. A close inspection of their molecular structure shows that their anti isomer should be sterically more hindered, due to some unavoidable interactions of the rhenium-bound phosphine with the diagonal carbonyl on Re(1) and Re(2).

Behavior of Adducts 2−4 in Solution. The addition of a good donor molecule such as PPh_3 to CH_2Cl_2 solutions of the adducts **2**−**4** restored the starting anion **1**, according to eq 8.[30−32] In agreement with previous

$$[Re_3\{\mu\text{-}M(PPh_3)\}(\mu_3\text{-}H)(\mu\text{-}H)_3(CO)_9(PPh_3)] + n PPh_3 \rightarrow [Re_3(\mu\text{-}H)_4(CO)_9(PPh_3)]^- + [M(PPh_3)_{n+1}]^+ \quad (8)$$

literature data,[31b] the complete conversion of the different adducts into **1** required different amounts of phosphine: 1 equiv of PPh_3 was sufficient for the gold adduct **3** and 2 equiv was necessary for the copper derivative **4**, while in the case of the silver adduct **2** a still higher amount was required, due to the formations of mixtures of the $[Ag(PPh_3)_3]^+$ and $[Ag(PPh_3)_4]^+$ cations (see Experimental Section).

Partial or complete cleavage of the interactions between **1** and the $[M(PPh_3)]^+$ cations resulted also from the simple dissolution of these adducts in a donor solvent such as acetone (eq 9). However, significant

$$[Re_3\{\mu\text{-}M(PPh_3)\}(\mu_3\text{-}H)(\mu\text{-}H)_3(CO)_9(PPh_3)] + Me_2CO \leftrightarrow [Re_3(\mu\text{-}H)_4(CO)_9(PPh_3)]^- + [M(PPh_3)(Me_2CO)]^+ \quad (9)$$

differences were observed in the behavior of the three adducts, as described in detail in the Supporting Information. The main features are discussed below.

In the case of copper, equilibrium 9 was completely driven to the right, as judged by ^1H NMR and IR spectra and by conductance measurements. Upon elimination of acetone, the adduct was quantitatively restored. In contrast, in the case of the gold derivative **3** equilibrium 9 implied the dissociation of a very small amount of **3** (ca. 5%). This equilibrium, which was attained immediately after dissolution, was further driven to the right by slower side reactions, which irreversibly consumed the gold cation, making only partial the reformation of **3** upon removal of acetone. Conductivity measurements suggested that **3** behaves as a weak electrolyte, but the aforementioned side reactions hampered the evaluation of equilibrium data.

Also for the silver adduct **2**, equilibrium 9 implied the fast dissociation of a very small amount of adduct. The reaction was completely reversed upon elimination of acetone. The extent of dissociation increased with dilution and on increasing the temperature. A plot of the reciprocal molar conductivity Λ against $c\Lambda$, according

(30) Extrusion of $[M(PPh_3)_n]^+$ groups by treatment of mixed transition metal−group 11 metal clusters with PPh_3 has been widely reported. See, for instance, refs 15 and 31. For extrusion from homonuclear clusters, see ref 32.

(31) (a) Alexander, B. D.; Boyle, P. D.; Johnson, B. J.; Casalnuovo, J. A.; Johnson, S. M.; Mueting, A. M.; Pignolet, L. H. *Inorg. Chem.* **1987**, *26*, 2547. (b) Evans, J.; Street, A. C.; Webster, M. *Organometallics* **1987**, *6*, 794.

(32) van der Velden, J. W. A.; Bour, J. J.; Bosman, W. P.; Noordik, J. H. *Inorg. Chem.* **1983**, *22*, 1913.

Table 3. Comparison of (Mean) Bond Parameters (Distances in Å and Angles in deg) for the Addition Derivatives $[Re_3\{\mu\text{-}M(PPh_3)\}(\mu_3\text{-}H)(\mu\text{-}H)_3(CO)_9(PPh_3)]$

	1	**2** (M = Ag)	**3** (M = Au)	**4m** (M = Cu)	**4o** (M = Cu)
Re(1)−Re(2)	2.797	2.840	2.859	2.827	2.826
Re(1,2)−Re(3)	3.214	3.199	3.192	3.199	3.196
Re(1,2)−M(1)		2.987	2.946	2.771	2.773
Re(1,2)−C(11,21)	1.90	1.93	1.94	1.93	1.91
Re(1,2)−C(12,22)	1.92	1.93	1.93	1.93	1.92
Re(1,2)−C(13,23)	1.92	1.91	1.91	1.91	1.92
Re(3)−P(1)	2.48	2.50	2.48	2.50	2.47
Re(3)−C(31,32)	1.92	1.91	1.92	1.92	1.92
Re(3)−C(33)	1.96	1.94	1.92	1.96	1.91
M(1)−P(2)		2.40	2.28	2.21	2.21
Re(3)−Re(1,2)−C(11,21)	158.5	157.6	158.0	158.4	158.1
Re(3)−Re(1,2)−C(12,22)	111.7	111.7	112.3	111.1	111.5
Re(3)−Re(1,2)−C(13,23)	95.6	92.4	91.4	91.8	92.7
Re(3)−Re(1,2)−M(1)		109.3	106.4	112.0	109.9
Re(1,2)−Re(2,1)−C(11,21)	96.9	99.4	99.0	100.6	99.1
Re(1,2)−Re(2,1)−C(12,22)	134.0	138.9	140.2	139.3	139.2
Re(1,2)−Re(2,1)−C(13,23)	135.0	130.6	128.2	130.6	130.8
Re(1,2)−Re(3)−P(1)	100.7	100.5	101.5	100.5	99.9
Re(1,2)−Re(3)−C(31,32)	107.4	107.4	106.4	107.2	107.6
Re(1,2)−Re(3)−C(32,31)	156.8	157.8	157.7	157.4	158.4
Re(1,2)−Re(3)−C(33)	80.8	79.5	79.4	80.3	80.5
[Re(1)Re(2)Re(3)]−[Re(1)Re(2)M(1)]		46.6	50.2	39.0	42.9

Table 4. Summary of Crystal Data, Data Collection Details, and Structure Refinement Parameters

	2	**3**	**4m**	**4o**
		Crystal Data		
formula	$C_{45}H_{34}AgO_9P_2Re_3$	$C_{45}H_{34}AuO_9P_2Re_3$	$C_{45}H_{34}CuO_9P_2Re_3$	$C_{45}H_{34}CuO_9P_2Re_3$
fw	1447.13	1536.23	1402.80	1402.80
cryst syst	monoclinic	orthorhombic	monoclinic	orthorhombic
space group	$P2_1/n$ (No. 14)	$P2_12_12_1$ (No. 19)	$P2_1/n$ (No. 14)	$P2_12_12_1$ (No. 19)
a (Å)	9.271(3)	13.710(3)	9.317(5)	13.659(3)
b (Å)	28.522(9)	18.183(5)	28.035(9)	18.135(5)
c (Å)	17.394(5)	18.528(5)	17.556(7)	18.529(5)
β (deg)	96.41(2)		96.91(4)	
V (Å^3)	4571(2)	4619(2)	4552(3)	4590(2)
Z	4	4	4	4
F(000)	2712	2840	2640	2640
density (g cm^{-3})	2.103	2.209	2.047	2.030
abs coeff (mm^{-1})	8.464	11.124	8.535	8.465
cryst descripn	yellow needle	orange prism	orange plate	orange prism
cryst size (mm)	0.10 × 0.08 × 0.03	0.34 × 0.14 × 0.14	0.38 × 0.38 × 0.08	0.34 × 0.32 × 0.26
		Data Collection		
diffractometer		Siemens SMART		
scan mode		ω		
θ range (deg)	$1.8 \le \theta \le 25.0$	$1.6 \le \theta \le 25.0$	$1.4 \le \theta \le 25.0$	$1.6 \le \theta \le 25.0$
index ranges	$-11 \le h \le 11$	$-16 \le h \le 16$	$-11 \le h \le 11$	$-16 \le h \le 16$
	$-33 \le k \le 33$	$-21 \le k \le 21$	$-33 \le k \le 33$	$-21 \le k \le 21$
	$-20 \le l \le 20$	$-22 \le l \le 22$	$-20 \le l \le 20$	$-22 \le l \le 22$
intensity decay (%)	none	4	none	none
abs corr		SADABS		
min rel transmissn factor	0.665	0.376	0.403	0.712
no. of measd rflns	39 419	40 720	39 297	40 310
no. of indep rflns	8052	8128	8032	8096
R_{int}, R_σ[a]	0.0542, 0.0413	0.0412, 0.0309	0.0519, 0.0336	0.0679, 0.0514
no. of rflns with $I > 2\sigma(I)$	6462	7655	6819	6648
		Refinement		
no. of data/params	8052/542	8128/542	8128/542	8096/542
weights (a)[b]	0.030	0.025	0.030	0.025
goodness of fit $S(F^2)$[c]	1.089	1.075	1.134	1.048
$R(F)$, $I > 2\sigma(I)$[d]	0.0304	0.0216	0.0285	0.0315
$R_w(F^2)$, all data[e]	0.0678	0.0514	0.0685	0.0664
largest diff peak, hole (e Å^{-3})	0.742, −0.747	0.669, −0.551	0.764, −0.808	0.489, −0.705

[a] $R_{int} = \sum|F_o^2 - F_{mean}^2|/\sum|F_o^2|$; $R_\sigma = \sum|\sigma(F_o^2)|/\sum|F_o^2|$. [b] $w = 1/[\sigma^2(F_o^2) + (aP)^2]$, where $P = (F_o^2 + 2F_c^2)/3$. [c] $S = [\sum w(F_o^2 - F_c^2)^2/(n-p)]^{1/2}$, where n is the number of reflections and p is the number of refined parameters. [d] $R(F) = \sum||F_o| - |F_c||/\sum|F_o|$. [e] $R_w(F^2) = [\sum w(F_o^2 - F_c^2)^2/\sum wF_o^4]^{1/2}$.

to the Ostwald dilution law,[33] provided a value of [1.5-(2)] × 10^{-4} M for the constant of equilibrium 9 at room temperature.

As to the kinetics of reaction 9, the equilibrium was attained very quickly for all of the three adducts. However, strong differences among them have been observed on the NMR time scale. In the case of the silver adduct **2**, the reversible dissociation of the $[Ag(PPh_3)]^+$ cation in acetone was so fast to broaden the resonances of **2** and of the anion **1** above 233 K (Figure 3) (still not completely dynamically averaged at room temperature). In contrast, the $[Au(PPh_3)]^+$ fragment did not show any

(33) Fuoss, R. M.; Accascina, F. *Electrolytic Conductance*; Interscience: New York, 1959.

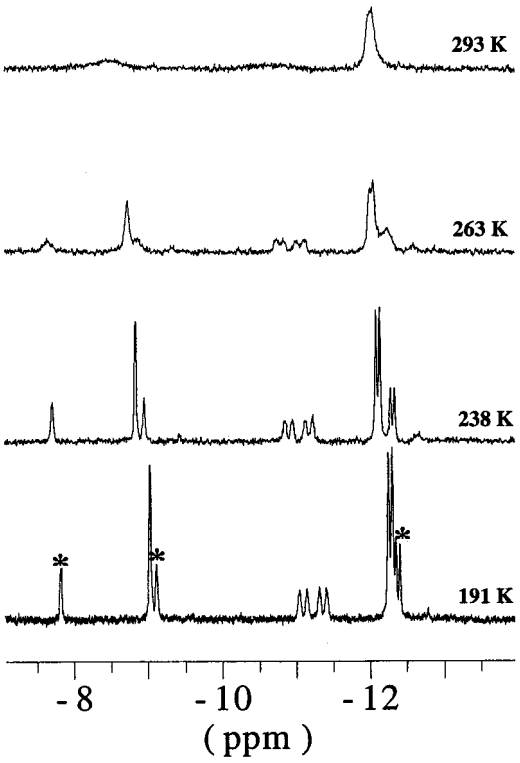

Figure 3. Variable-temperature ^{1}H NMR spectra (hydridic region) of a 4.6×10^{-4} M solution of **2** (isolated crystals) in acetone-d_6. The peaks labeled with asterisks are due to the anion **1**, originating from dissociation of the adduct in the diluted acetone solution.

lability in acetone: no exchange between **3** and **1** was revealed by EXSY experiments, even at room temperature.

The exchange between the silver adduct **2** and **1** occurs also in CD_2Cl_2, even if with a much slower rate (the resonances of the two species being sharp up to room temperature; Figure 4a). In passing, we observe that the cross-peak between the Ag-coupled signal of **2** and the hydridic resonance of **1** at intermediate field (δ −8.9) completed the attribution of the resonances of **1**, allowing the identification of the resonance of **1** due to the hydride syn with respect to the phosphine ligand.

Lability in CD_2Cl_2 was observed also for the copper derivative **4** (but not for the gold adduct **3**, as expected due to its inertness in acetone). However, the exchange pattern revealed by 2D experiments concerning **4** (with mixing times in the range 0.3−0.8 s) was more complex than that of **2**. Indeed the hydrides H_a and H_b of both species **1** and **4** had exchange cross-peaks with all the other resonances of intensity 1, as shown in Figure 4b. Since in **1** alone the exchange between H_a and H_b does not occur, on the NMR time scale of this experiment, such exchange must be mediated by the H_a/H_b exchange within adduct **4**. A 2D EXSY experiment, performed with a shorter mixing time (0.05 s), supported this view, since it showed exchange cross-peaks only between the H_a and H_b signals of **4** (Figure 4c). This exchange must occur through an intramolecular pathway, since any dissociative process would imply **4**/**1** exchange, not observed with this shortest mixing time. A planar "lozenge" structure, with H_a and H_b in equivalent positions, bridging on the two Re−Cu interactions, might constitute a reasonable transition state for this

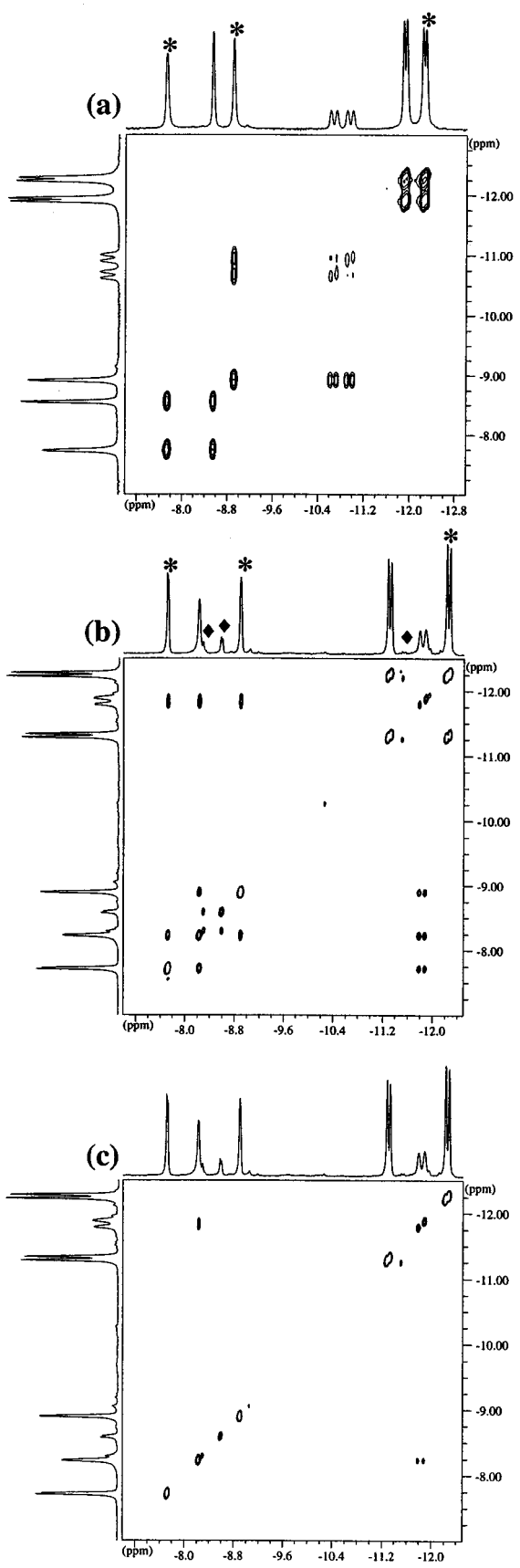

Figure 4. ^{1}H 2D-EXSY experiments acquired at room temperature in CD_2Cl_2 on equimolar mixtures of **1** and the silver or copper adducts, respectively, in the hydridic region: (a) **1** and **2**, $\tau_m = 0.3$ s (the asterisks mark the signals of **1**); (b) **1** and **4**, $\tau_m = 0.8$ s(the diamonds mark unidentified impurities); (c) **1** and **4**, $\tau_m = 0.05$ s.

exchange. However, further investigation into this unusual process is in progress. At longer times the dissociation of the $[Cu(PPh_3)]^+$ fragment causes the **4**/**1** exchange, as observed for the silver adduct **2**.

Conclusions. The results reported above have demonstrated that the hydrides of the unsaturated Re(μ-H)$_2$Re moiety are the sites of electrophilic attack by the $[M(PPh_3)]^+$ cations. However, different from what occurs with other electrophiles, no hydride (eqs 1 and 2) or electron (eq 3) transfer takes place, and the reactions stop at the initial stage: i.e., the formation of the hydride-bridged acid−base adduct. This likely results both from the low tendency of group 11 atoms to give hydridic derivatives and from the stabilization of the $Re_3H^-\cdots MPPh_3^+$ interactions for the formation of the butterfly Re_3M metal skeletons. Moreover, the cleavage of the adducts **2**−**4** by reaction with phosphines (eq 8) demonstrated that in this case it is the $[M(PPh_3)]^+$ cation that would act as a scavenger of the L′ ligands, and not the Re_3 unsaturated fragment, as required by eq 1.

The M(PPh$_3$) fragment can be considered to be isolobal with a hydrido ligand,[18,19] and experimentally it has been found that in almost all compounds containing just one Au(PPh$_3$) fragment this fragment occupies a position similar to that of the hydrido ligand in the related hydrido derivative.[8,19] On these grounds the adducts **2**−**4** could provide a model of the kinetic product resulting from the attack of the proton on the hydride of the unsaturated anions $[Re_3(\mu\text{-}H)_4(CO)_9L]^-$. From this point of view these adducts should be formulated as triangular clusters containing a bridging η^2-HM(PPh$_3$) ligand,[14] isolobally analogous to an (until now unknown) bridging η^2-H_2 ligand.

The nature of these adducts in solution requires a short discussion. In principle they could be viewed either as Lewis acid−base adducts or as tight ionic couples between the group 11 cations and the triangular cluster anion. Accordingly, the (partial or complete) dissociation in acetone could be attributed either to the Lewis basicity of the solvent or to its high dielectric constant, favoring the cleavage of the ionic couple. We observed that the dissociation of the copper adduct was complete not only in acetone but also in a donor solvent with a low dielectric constant such as THF, while it was negligible in a solvent such as nitromethane, with a high dielectric constant but a low donor capability. This rules out the hypothesis of an ionic interaction. Moreover, the high values of the coupling constants observed in CD_2Cl_2 solution between the triply bridging hydride and the ^{31}P atoms of the $[M(PPh_3)]^+$ groups (and with the Ag isotopes in the case of compound **2**) fully support the idea of a true covalent interaction.

However, such interactions must be considered quite weak, since a solvent with a donor power as poor as that of acetone is sufficient to extrude (partially or completely) the $[M(PPh_3)]^+$ cations. A similar behavior was previously observed for other weak adducts, such as those between the Mn(μ-H)$_2$Mn moiety and $[M(PPh_3)]^+$.[17,34] The weakness of such adducts is substantiated also by the X-ray structures, which show little perturbation with respect to the parent anion **1**. The position of equilibrium 9 cannot be taken as a measure of the strength of the interaction (copper is weaker than silver and gold), since such a position depends also on the strength of the M−acetone bond, whose formation drives the cleavage of the adducts.

The $[M(PPh_3)]^+$ cations exhibit different labilities: the gold derivative is inert even in acetone, while the copper and silver adducts are labile (on the NMR time scale) also in CH_2Cl_2, at room temperature. Examples of intermolecular exchange of $[M(PPh_3)]^+$ moieties in solution have already been reported,[8] and also the fact that gold complexes tend to be less dynamic has been previously pointed out.[31b,35]

In the related adduct between $[Mn_2(\mu\text{-}H)_2(CO)_6(\mu\text{-}dppm)]$ and $[Ag(PPh_3)]^+$, Riera et al. observed the shift of the cation between the two hydrides of the Mn(μ-H)$_2$Mn moiety and suggested a dissociative pathway for such exchange.[17] In the present case, such a shift would afford the anti isomer, which is expected to be less stable, for steric reasons, and it is not observed. The exchange between the hydrides H_a and H_b observed for the copper derivative **4** most likely involves a different, intramolecular, mechanism. Further investigation on this subject is in progress.

Experimental Section

The reactions were performed under nitrogen, using the Schlenk technique, and solvents were deoxygenated and dried by standard methods. Literature methods were used for the preparation of $[Re_4(\mu_3\text{-}H)_4(CO)_{12}]$,[36] [PPh$_4$](**5**),[29] $[Au(PPh_3)Cl]$,[37] and $[Cu(PPh_3)_2NO_3]$.[38] $[Cu(CH_3CN)_4][BF_4]$ was obtained by a literature method,[39] using HBF_4 instead of HPF_6. [PPh$_4$](**1**) was obtained quantitatively by treating the $[PPh_4]^+$ salt of **5** with a stoichiometric amount of PPh$_3$ in CH_2Cl_2 at room temperature. PPh$_3$ (Merck) and AgOTf (Aldrich) were used as received. The NMR spectra were acquired on Bruker AC200 and DRX300 spectrometers, the former equipped with an external BSV3 unit. IR spectra were acquired on a Bruker Vector22 FT spectrometer. Microanalyses were performed at the microanalytical laboratory of the University of Milan.

Synthesis of $[Re_3\{\mu\text{-}Ag(PPh_3)\}(\mu_3\text{-}H)(\mu\text{-}H)_3(CO)_9(PPh_3)]$ (2). A solution of 32.4 mg (0.0229 mmol) of [PPh$_4$](**1**) in CH_2Cl_2 (5 mL) was treated at room temperature with 1.53 mL of an equimolar solution (0.015 M) of PPh$_3$ and AgOTf in CH_2Cl_2/acetone (3/1). The solution instantaneously became dark yellow, and IR monitoring showed the quantitative formation of adduct **2**. Addition of freshly distilled Et_2O to the solution (after reduction of the volume to ca. 1 mL, under vacuum) caused the precipitation of an off-white solid, identified as [PPh$_4$]OTf. The bright yellow solution was separated and evaporated to dryness. Crystallization of the residue from CH_2Cl_2/*n*-hexane afforded a yellow solid (isolated yield 18.5 mg, 0.0128 mmol, 56%, after drying in vacuo). Anal. Calcd for $C_{45}H_{34}AgO_9P_2Re_3$: C, 37.32; H, 2.37. Found: C, 37.4; H, 2.4. Single crystals suitable for X-ray analysis were obtained by low-temperature (−25 °C), slow diffusion of *n*-hexane into a concentrated CH_2Cl_2 solution. IR and NMR data: see Table 1.

^{1}H−^{31}P HMQC experiments (7.05 T, 300 K), optimized for $J_{HP} = 4$ and 15 Hz, were performed on a solution prepared by

(34) No reaction was observed between $[Mn_2(\mu\text{-}H)_2(CO)_6(\mu\text{-}dppm)]$ and $[Au(PPh_3)]^+$ in THF, but it did occur upon removal of the solvent and dissolution in CH_2Cl_2.[17]

(35) Albinati, A.; Lehner, H.; Venanzi, L. M.; Wolfer, M. *Inorg. Chem.* **1987**, *26*, 3933.
(36) Johnson, J. R.; Kaesz, H. D. *Inorg. Synth.* **1978**, *18*, 60.
(37) Bruce, M. I., Nicholson, B. K.; Bin Shawkataly, O. *Inorg. Synth.* **1989**, *26*, 324.
(38) Gysling, H. J. *Inorg. Synth.* **1979**, *19*, 92.
(39) Kubas, G. J. *Inorg. Synth.* **1979**, *19*, 90.

dissolving 8.0 mg (0.0055 mmol) of **2** in 0.5 mL of CD_2Cl_2. These experiments showed that (i) H_a has a (small) correlation only with the rhenium-bound phosphorus P(1) due to the coupling measured in the 1D spectrum (see Table 1), (ii) the triply bridging hydride H_b has a small correlation (not sizable in the 1D spectrum) also with P(1), in addition to the strong correlation with P(2), and (iii) the two hydrides H_c bridging on the lateral edges have a small correlation (not sizable) also with P(2), in addition to the strong coupling with P(1).

Synthesis of $[Re_3\{\mu\text{-}Au(PPh_3)\}(\mu_3\text{-}H)(\mu\text{-}H)_3(CO)_9(PPh_3)]$ (3). A solution of $Au(PPh_3)Cl$ (26.8 mg, 0.0542 mmol) in CH_2Cl_2 (1 mL) was treated with 380 μL of a 0.1454 M solution of AgOTf in acetone. The precipitate (AgCl) was separated by slow decantation, and 340 μL of the solution (about 0.0134 mmol of $[Au(PPh_3)]^+$) was added to a solution of $[PPh_4]$(**1**) (19.0 mg, 0.0134 mmol) in CH_2Cl_2 (3 mL). The color changed immediately from yellow to orange, and IR monitoring showed the quantitative formation of **3**. The solution was treated as described in the previous synthesis, affording orange microcrystals of **3** (15 mg, 0.0097 mmol, 73% isolated yields after crystallization from CH_2Cl_2/*n*-hexane). Anal. Calcd for $C_{45}H_{34}AgO_9P_2Re_3$: C, 35.16; H, 2.23. Found: C, 35.4; H, 2.4.

Synthesis of $[Re_3\{\mu\text{-}Cu(PPh_3)\}(\mu_3\text{-}H)(\mu\text{-}H)_3(CO)_9(PPh_3)]$ (4). (a) From the Anion 1. A CH_2Cl_2 solution of $[PPh_4]$(**1**) (14.4 mg, 0.0102 mmol) was treated at room temperature with 425 μL of an equimolar solution (0.024 M) of $[Cu(CH_3CN)_4][BF_4]$ and PPh_3 in CH_2Cl_2. The solution turned dark yellow. The reaction mixture was stirred for about 5 min, concentrated to a small volume, and treated with Et_2O, causing the precipitation of $[PPh_4][BF_4]$. The yellow solution was separated and evaporated to dryness, and the residue was crystallized from CH_2Cl_2/*n*-hexane. The yellow solid so obtained contained again some impurity, on the basis of NMR analysis (the main signals being a doublet at -6.43 ppm, $J_{HP} = 16$ Hz, and two singlets at -8.60 and -12.67 ppm; overall integrated intensity ca. 20% of the whole intensity in the hydride region). Pure **4** was obtained by slow diffusion of *n*-hexane into a concentrated CH_2Cl_2 solution (4.3 mg, 0.003 mmol, 29%).

(b) From the Anion 5. A solution of $[Re_4(\mu_3\text{-}H)_4(CO)_{12}]$ (42.9 mg, 0.0346 mmol) in CH_2Cl_2 (6 mL) was treated with 250 μL of acetone at room temperature. The solution was stirred for ca. 60 min until the red-brown color completely disappeared and the solution became bright yellow. Addition of $[Cu(PPh_3)_2(NO_3)]$ (22.7 mg, 0.0346 mmol) caused a sudden change of the color at first to red and then to yellow. The product was purified by chromatography on a silica gel column, by elution with CH_2Cl_2/*n*-hexane (1/1). Concentration under vacuum afforded a yellow precipitate, which was isolated and crystallized by slow diffusion of *n*-hexane into CH_2Cl_2 solution (21.0 mg of crystals, 0.0149 mmol, isolated yield 43%). Anal. Calcd for $C_{45}H_{34}AgO_9P_2Re_3$: C, 38.50; H, 2.44. Found: C, 38.4; H, 2.5.

Reactions of Adducts 2−4 with PPh_3. (a) Adduct 2. A solution of **2** (13.8 mg, 0.0095 mmol) in CD_2Cl_2 (0.5 mL) was treated at room temperature with 2.5 mg of PPh_3 (0.0095 mmol). The ^1H NMR spectrum (183 K) showed the hydridic resonances of both **2** and **1**, in a ca. 1:1 ratio. ^{31}P NMR showed, besides the signals of **2** and **1**, also two doublets of doublets (ratio ca. 1.2:1, one component of the lowest field doublet partially overlapping with signals of **1** and **2**), attributable respectively to $[Ag(PPh_3)_4]^+$ (δ 5.68, $J(^{107}AgP) = 223$ Hz) and $[Ag(PPh_3)_3]^+$ (δ ca. 11.5, $J(^{107}AgP) =$ ca. 300 Hz).[40] Addition of another 1 equiv of PPh_3 did not cause the complete disappearance of **1** (residual amount ca. 25%), and ^{31}P NMR showed the increase of the signal of $[Ag(PPh_3)_4]^+$ with respect to that of $[Ag(PPh_3)_3]^+$ (ratio ca. 2:1).

(b) Adduct 3. The ^1H NMR spectrum (300 K) of a $CDCl_3$ solution containing **3** (8.0 mg, 0.0052 mmol) and a slight excess of PPh_3 (2.0 mg, 0.0078 mmol) showed the quantitative formation of **1**. ^{31}P NMR showed, besides the signal of **1**, also a broad signal at δ 29.2 ppm, attributable to dynamic averaging[32] of the signals of free phosphine and of the $[Au(PPh_3)_2]^+$ cation (δ 45.4).[41]

(c) Adduct 4. Addition of 1 equiv of PPh_3 (8.5 μL of a 0.126 M solution of PPh_3 in CD_2Cl_2) to a solution of **4** (1.4 mg, 0.001 mmol) in CD_2Cl_2 (0.5 mL) caused the formation of an equimolar mixture of **1** and **4**. Addition of another 1 equiv of PPh_3 completed the conversion of **4** into **1**. ^{31}P NMR (183 K) showed, besides the signal of **1**, also a signal at δ 1.87 ppm, attributable to the $[Cu(PPh_3)_3]^+$ cation.[31b]

^1H 2D NMR Investigation of the Behavior of Adducts 2−4 in CD_2Cl_2 in the Presence of an Equimolar Amount of Anion 1. Three samples were prepared by dissolving in CD_2Cl_2 roughly equimolar amounts (typically 7×10^{-3} mmol) of $[PPh_4]$(**1**) and of one of the adducts **2**−**4**. ^1H 2D EXSY phase-sensitive experiments (7.05 T)[42] were performed for each sample at 300 K with different mixing times (τ_m) and relaxation-delay values. For both the Ag and Cu derivatives, the experiments performed with $\tau_m = 0.3$ s showed chemical exchange with compound **1**, while for the Au derivative, even with the mixing time $\tau_m = 0.8$ s, no exchange was detected. For the copper derivative **4**, experiments with $\tau_m = 0.8$ and 0.05 s were also performed. For the observation of NOE effects between the hydrides and the phenylic hydrogens of the phosphines (as described above) further experiments were performed on the mixture of **1** and **2**, on using longer relaxation delays and mixing times (2.0 and 1.0 s, respectively). Typically 16 fid's were acquired on a spectral width of 7184 Hz (4496 Hz for **4**) using 1K data points for each of the 256 experiments. Shifted sine-bell functions were applied in both dimensions before Fourier transform and after zero-filling to 1K in F1.

X-ray Diffraction Structural Analysis. (a) Collection and Reduction of X-ray Diffraction Data. Suitable crystals were mounted in air on a glass fiber tip onto a goniometer head. Single-crystal X-ray diffraction data were collected on a Siemens SMART CCD area detector diffractometer, using graphite-monochromated Mo Kα radiation ($\lambda = 0.710\,73$ Å) at room temperature (293(2) K). Unit cell parameters were initially obtained from about 100 reflections ($5° < \theta < 20°$) taken from 45 frames collected in three different ω regions and eventually refined against a large amount of reflections (about 8000). A full sphere of reciprocal space was scanned by 0.3° ω steps, collecting 1800 frames each at 40 s exposure and keeping the detector at 3.88(2) cm from the sample. Intensity decay was monitored by recollecting the initial 100 frames at the end of data collection and analyzing the duplicate reflections. The collected frames were processed for integration (SAINT[43]); an empirical absorption correction was made on the basis of the symmetry-equivalent reflection intensities collected (SADABS[44]). Crystal data and data collection parameters are summarized in Table 4.

(b) Structure Solution and Refinement. The structures were solved by direct methods (SIR97[45]) and subsequent Fourier synthesis; they were refined by full-matrix least squares on F^2 (SHELX97[46]) using all reflections. Scattering factors for neutral atoms and anomalous dispersion corrections were taken from the internal library of SHELX97. Weights were assigned to individual observations according to the

(40) Alyea, E. C.; Malito, J.; Nelson, J. H. *Inorg. Chem.* **1987**, *26*, 4294.

(41) Sykes, A. G.; Mann, K. R. *J. Am. Chem. Soc.* **1990**, *112*, 7247.

(42) Bodenhausen, G.; Kogler, H.; Ernst, R. R. *J. Magn. Reson.* **1984**, *58*, 370.

(43) SAINT; Bruker AXS, Madison, WI, 1993−1999.

(44) Sheldrick, G. M. SADABS: Program for Empirical Absorption Correction; University of Göttingen, Göttingen, Germany, 1996.

(45) Altomare, A.; Burla, M. C.; Camalli, M.; Cascarano, G. L.; Giacovazzo, C.; Guagliardi, A.; Moliterni, A. G. G.; Polidori, G.; Spagna, R. *J. Appl. Crystallogr.* **1999**, *32*, 115.

(46) Sheldrick, G. M. SHELX97: Program for Crystal Structure Refinement; University of Göttingen, Göttingen, Germany, 1997.

formula $w = 1/[\sigma^2(F_o^2) + (aP)^2]$, where $P = (F_o^2 + 2F_c^2)/3$; the parameter a was chosen to give a flat analysis of variance in terms of F_o^2. Anisotropic displacement parameters were assigned to all non-hydrogen atoms. Hydride ligands were initially evidenced by a difference Fourier map; their positions were in agreement with the local stereogeometry around the metal centers. They were eventually constrained in more accurate positions (calculated employing the program HYDEX,[47] with $d_{Re-H} = 1.85$ Å for both edge- and face-bridging ligands) and refined with a common (refined) isotropic displacement parameter. Hydrogen atoms of the triphenylphosphine ligands were placed in idealized positions ($d_{C-H} = 0.93$ Å) and refined riding on their parent atom with an isotropic displacement parameter 1.2 times that of the pertinent carbon atom. For compounds **3** and **4o** the correctness of the absolute structure was checked, and the Flack parameters[48] for the correct enantiomer were 0.007(6) and 0.007(9), respectively. The final difference electron density maps showed no features of chemical significance, with the largest peaks lying close to the metal atoms. Final conventional agreement indexes and other structure refinement parameters are listed in Table 4.

(47) Orpen, A. G. *J. Chem. Soc., Dalton Trans.* **1980**, 2509.
(48) Flack, H. D. *Acta Crystallogr.* **1983**, *A39*, 876.

Acknowledgment. This work has been supported by the Italian CNR (CSMTBO) and by the MIUR (Project Metal Clusters: Basic and Functional Aspects). Thanks are due to Mr. Pasquale Illiano for the careful acquisition of the 2D NMR data.

Supporting Information Available: Text giving details on the reaction of **1** with $Cu(NCMe)_4^+/PPh_3$ monitored in the NMR tube and on the behavior of adducts **2**−**4** in acetone solutions, conductivities of acetone solutions of **2** and **4** (Table S1), time evolution of **3** in acetone (Figure S1); ORTEP drawings for **4m** and **4o** (Figures S2 and S3), and final atomic coordinates, anisotropic displacement parameters, and tables giving all bond distances and angles for **2**, **3**, **4m**, and **4o**. This material is available free of charge via the Internet at http://pubs.acs.org.

OM0200252